

# TOWARDS THE DESCRIPTION OF LONG TERM SELF CONSISTENT EFFECTS IN SPACE CHARGE INDUCED RESONANCE TRAPPING

G. Franchetti<sup>†</sup>, I. Hofmann<sup>†</sup>, S. Machida<sup>\*</sup>

<sup>†</sup>GSI, 64291 Darmstadt, Germany

<sup>\*</sup>CCLRC/RAL/ASTeC, Chilton, Didcot, Oxon, U.K.

## Abstract

In recent studies the effect of the space charge induced trapping has been shown relevant for long term storage of bunches. There the mechanisms of emittance growth and beam loss have been studied for frozen bunch particle distribution. However, when beam loss or halo density are large enough, this approximation has to be reconsidered. We present here a first study on the effect of self-consistency in frozen models as intermediate step towards fully 2.5 and 3D simulations.

## INTRODUCTION: THE CHALLENGES OF THE HIGH INTENSITY BEAMS

The increase of the beam intensity is an essential requirement for basic research of several new projects. Basic issues are beam quality control (control of the emittance increase) and beam loss. For example in the SNS project proton bunched beams are stored for 1000 turns in a four fold storage ring reaching a space charge tuneshift of  $\Delta Q = 0.15/0.2$  [1]. In this project the beam loss control is very restrictive:  $\Delta N/N = 10^{-4}$  [2]. In the JPARC project the intensity of beams leads to tuneshifts of the order of  $\Delta Q = 0.17 - 0.28$ . Proton bunched beams should be stored for  $2.5 \times 10^4$  turns [3]. The beam loss control allows here 4.5% beam loss. At GSI the SIS100 synchrotron [4] of FAIR project is foreseen to deliver  $U^{+28}$  at an intensity of  $6 \times 10^{11}/s$  with  $\Delta Q = 0.2$ . This goal is reached by injecting 4 bunches from SIS18 in 2 different cycles. The beam loss control is of 5% (1W/m hand-on maintenance). The beam loss control will be obtained as a trade-off between collimation system, magnet field quality, and resonance correction system. However, as the storage time in SIS100 is of one second ( $\sim 2 \times 10^5$  turns), during the storage the bunch has the time to experience the space charge repulsion, the lattice nonlinearities, and the synchrotron motion. The latter plays, jointly with the space charge, an essential role in determining beam loss. This complex beam dynamics has been addressed in some detail in [5].

## Computational challenges

A simple estimation of the computational load for predicting the beam loss evolution and distribution along the SIS100 reveals challenging aspects for standard PIC codes. In fact, taking a PIC grid resolution of the beam of  $\pm 10$  grids, and considering a ratio beam pipe over beam size of 6, we obtain a transverse grid of  $125 \times 125$ . Keeping the

same number of grid points longitudinally we easily obtain  $\sim 10^4$  grid cells covering the beam. The finite number of macro-particles into each grid cell is responsible for statistical fluctuations and artificial emittance growth [6]. Estimates from [7] suggest that few % emittance growth in a 2D coasting beam with  $\Delta Q/Q \sim 0.01$  and  $\epsilon_x = 50$  mm-rad requires a control of the noise due to statistical fluctuation better than 1% for long term simulation, that is more than  $10^4$  particles per grid cell should be foreseen. This rough estimates easily leads to  $10^8$  macro-particles needed to simulate the space charge in a bunched beam. The requirements on the integration step are important as well: in a constant focusing lattice 20 integration kicks per betatron wavelength allows to obtain an integrated dynamics, which has a relative error less than 0.1% on the tuneshift. For a typical tune of SIS100 as  $Q_x \sim 18$ , we find 360 integration steps. The overall computational load is severe as over  $2 \times 10^5$  turns  $10^8$  macro-particles should be integrated in  $10^8$  integration steps. In this simulation condition the long term effect of the *modeling adopted* is crucial.

## THE ROLE OF COMPUTER MODELING

The number of existing accelerator codes is considerable [8], and each of them is specialized in some area of interest of the main code author or of the community, which the code serves. However, when the complexity of the phenomena under study is considerable and the understanding of the mechanisms involved is in progress, the role of the modeling becomes critical. In fact in regimes of high non-linearity, implicit assumptions deriving from the modelization may affect the outcome of simulations. The validation of the computer modeling is therefore an essential step towards the simulation of highly complex system such as the long term storage of a high intensity bunch. The validation process can follow 2 steps (see also Fig. 1). A benchmarking/validation of the main space charge codes has been performed for the Montague resonance [9].

- code-code benchmarking: results from different codes simulating the same system are compared. The goal of this step is to reach confidence that the modeling is correct;
- experiment-code benchmarking: here the computer modeling is used to reproduce the observables measured in an experiment. It is therefore validated, that the physics in the model "correctly" fits the physical problem under study.

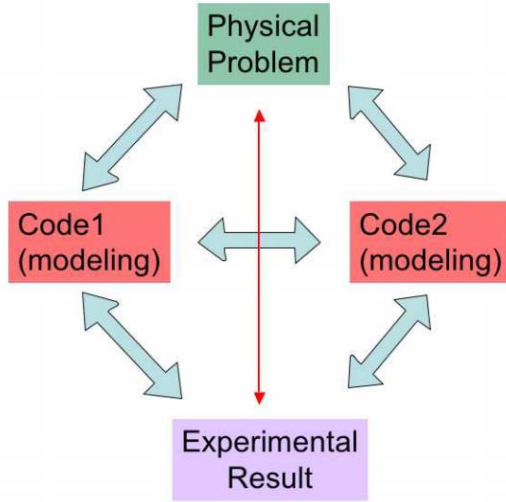


Figure 1: In this schematic is shown the role of modeling in the simulation of complex systems.

## MODELING OF THE PHYSICS IN A HIGH INTENSITY BUNCH

### A simplified approach

We describe below the elements of a simplified 1D model which allow a discussion on the relevant high intensity effects during the long term storage. The main assumption used here is that the bunch distribution is frozen.

- The AG structure of the lattice is substituted by a constant focusing lattice. The equation of motion becomes  $x'' + (Q_{x0}/R)^2 x = 0$ , where  $Q_{x0}$  is the machine bare tune and  $R$  the ring radius.
- We then assume that the bunch distribution is Gaussian in all 3 dimensions

$$\rho(x, y, z) \propto \exp\left(-\frac{x^2}{2\sigma_x^2} - \frac{y^2}{2\sigma_y^2} - \frac{z^2}{2\sigma_z^2}\right). \quad (1)$$

This distribution is deriving from a 6D matched bunch into a 3 dimensional focusing structure. Also  $\sigma_x, \sigma_y, \sigma_z$  are the  $x, y, z$  bunch rms sizes. This type of distribution is realistic in absence of space charge. When space charge is weak ( $\Delta Q/Q \sim 1\%$ ), the distribution form assumed in Eq. 1 still remain a good approximation.

- We introduce the lattice nonlinear component via symplectic kicks of the form

$$\begin{pmatrix} x \\ x' \end{pmatrix} \rightarrow \begin{pmatrix} x \\ x' + k_n x^n \end{pmatrix} \quad (2)$$

- For long bunches, which in normal operation condition can have an aspect ratio  $\sigma_x/\sigma_z \sim 10^{-3}$ , the transverse space charge can be computed assuming that the

bunch is locally (at a given  $z$ ) similar to a coasting beam. For the purpose of this model we further assume, for simplicity, that the bunch has equal transverse axis. In this case the electric field in units of the equation of motion can be computed by

$$E_x(x, y, z) = K e^{-z^2/(2\sigma_z^2)} \frac{x}{r^2} \left[1 - e^{-r^2/(2\sigma_x^2)}\right]. \quad (3)$$

Here  $K$  is the beam perveance. Note that in this equation the term  $r = \sqrt{x^2 + y^2}$  should be understood as  $r = x$ , in fact as we discuss a 1D model, we should keep the coordinate in the  $y$ -plane to zero. A better modeling of the space charge in which the transverse aspect ratio is taken into account is found in the classical integral expression [10]

$$\mathcal{E}_x = x \frac{Q}{2} \int_0^\infty \frac{\hat{n}(\hat{T}) ds}{(\sigma_x^2 + s)^{3/2} (\sigma_y^2 + s)^{1/2} (\sigma_z^2 + s)^{1/2}}, \quad (4)$$

where  $\hat{T} = x^2/(\sigma_x^2 + s) + y^2/(\sigma_y^2 + s) + z^2/(\sigma_z^2 + s)$ . In [11] this expression is expanded in power series to provide an space charge algorithm which is implemented into the MICROMAP library.

- The integration scheme of the equation of motion is standard: the space charge is introduced by kicks of the form as in Eq. 2 with the substitution  $k_n x^n \rightarrow E_x \Delta s$ , where  $\Delta s$  is the integration steps. The number of integration steps per turn is taken as  $20 \times Q_x$ .

We apply this simplified model to the SIS18, where  $R = 34.4$  m, and take  $Q_{x0} = 4.35$ , and  $Q_{z0} = 10^{-3}$ . We excite a 3rd order resonance  $3Q_x = 13$  via a single sextupole with  $k_2 = 0.1 \text{ m}^{-2}$ . In Fig. 2a is shown the evolution of the single particle emittance  $\epsilon_x$  of a test particle with initial coordinates  $x = 1.5\sigma_x$ , and  $x = x' = y = y' = z' = 0$  and  $z = 3\sigma_z$ . Note the initial scattering of  $\epsilon_x$ , which stems from an incomplete trapping as the islands are crossing the particle's orbit in a non-adiabatic condition. The scattering is responsible for a nonlinear diffusion (see in Fig. 2b the dense accumulation of orbits at small radii). When the diffusion has brought the particle to large amplitudes, the crossing of the island through the particle orbit gets closer to an adiabatic crossing and trapping into islands occurs. In Fig. 2a this is visible in the large jumps of  $\epsilon_x$ . In Fig. 2b the path of the particle orbit in the Poincaré section is shown: note that the region explored by the test particle is very wide with respect the the rms beam size (the  $x$  axis is in units of  $\sigma_x$ ). when a full bunch is considered, this region becomes a halo. On the left the shadowed region represents an example of a forbidden region, which may arise from the presence of a mechanical aperture limitation in the ring. Due to the scattering/trapping of the invariant, the particle eventually reaches the forbidden area and get lost. When the mechanical aperture is further limited by the dynamic aperture (DA), the beam loss mechanisms is essentially the same, with the difference that the intercep-

tion of the halo with the DA creates a chaotic region. and the particle extraction is enhanced by chromaticity.

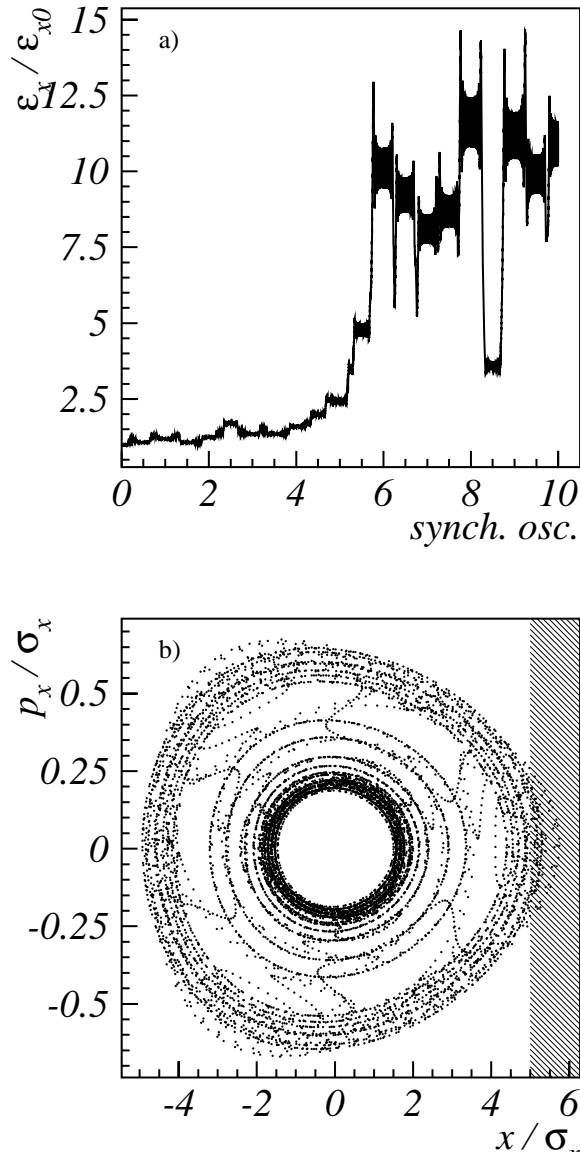


Figure 2: a) Single particle emittance evolution rescaled with the initial emittance; b) Poincaré section of one particle. The

### The role of the chromaticity

A detailed 2D modeling of the effect of a long term storage of a high intensity bunch is reported in [12]. An important result is that the halo extension goes to infinity when the bare tune approaches the resonance from above (in this example  $Q_{x0} > Q_{xr}$  and  $Q_{x0} \rightarrow Q_{xr}$ ). When the chromaticity is present (here natural chromaticity) the particle tune is effected from momentum gain or a momentum loss. Let's consider the particles in the bunch of given maximum off momentum  $\delta p/p$ . During the synchrotron

oscillations an extra tune modulation is introduced by the chromaticity. If the bare tune is  $Q_{x0}$ , when the particle is in the center of the bunch ( $z = x = 0$ ), the single particle tune is  $Q_x = Q_{x0} \pm \Delta Q_{x,chr} - \Delta Q_{x,sc}$ . The sign  $\pm$  is related to the loss/gain of momentum during the synchrotron oscillations, and  $\Delta Q_{x,chr} = -Q_{x0} \delta p/p$  represents the maximum tune variation due to the chromaticity for the particles with maximum off-momentum  $\delta p/p$ . If the effective "bare tune"  $\tilde{Q}_x = Q_{x0} - \Delta Q_{x,chr}$  is below the resonance, then during one synchrotron oscillation there will be a longitudinal amplitude  $z^*$  such that  $\tilde{Q}_x$  sits on the 3rd order resonance bringing consequently the fixed points (and the halo) to infinity. This argument can be applied to all particles in the bunch that have effective "bare tune"  $\tilde{Q}_x = Q_{x0} - \Delta Q_{x,chr}$  below the resonance. The number of those particles is function of  $Q_{x0} - Q_{xr}$ . The overall effect is that the chromaticity leads to a beam loss stop-band as large as  $(\Delta Q_{x,chr})_{spread}$  for the bunch.

## VALIDATION

### Code-code benchmarking

As previously discussed the code-code benchmarking plays an important role in validating codes. For this reason a code-code benchmarking has been initiated between MICROMAP and SIMPSONS on the modeling of the dynamics of a bunched beam in SIS18 [13]. The bunch in-

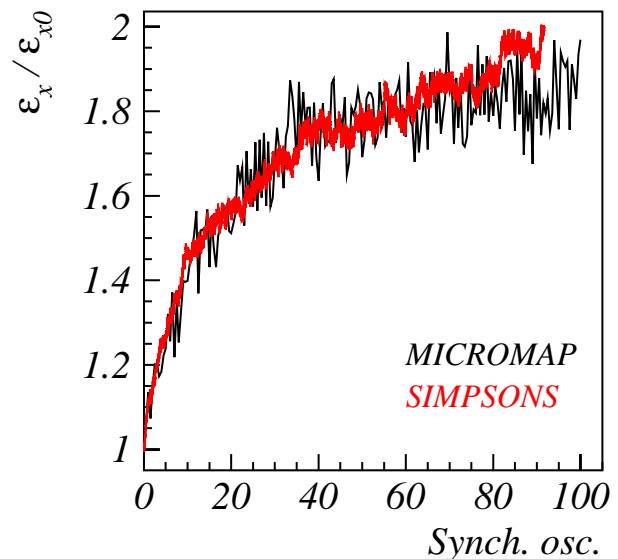


Figure 3: Rms emittance evolution as predicted by MICROMAP and SIMPSONS.

tensity was adjusted to obtain a tuneshift of  $\Delta Q_x = 0.1$ . The transverse sizes are  $X_{rms} = Y_{rms} = 5$  mm. One synchrotron oscillation takes 1000 turns. A 3rd order resonance was excited by a single octupole in the linear lattice. The integrated strength is  $K_2 = 0.2 \text{ m}^{-2}$ . The benchmark

was performed in many steps to reach confidence that the accelerator model and the initial condition of the simulations were the same in both codes. In Fig. 3 is shown the result of the rms emittance growth versus time obtained from the two codes for  $Q_{x0} = 4.36$  over 100 synchrotron oscillations. The agreement reached is excellent on the time-scale simulated.

### Experiment-code benchmarking: the CERN-PS measurements

In the experimental campaigns undertaken at the CERN-PS these high intensity effects have been explored in well experimental controlled conditions. The main parameters of the measurements are  $\Delta Q_x = 0.075$ , storage time of  $4.5 \times 10^5$  turns. The rms momentum spread of the beam is  $\Delta p/p = 1.5 \times 10^{-3}$  (for more information on the experiment see [5]). Figure 4 summarizes the experimental findings and the simulation results. The green curve shows the simulation beam intensity after 1 second storage. The reproduction of the beam loss (16% maximum

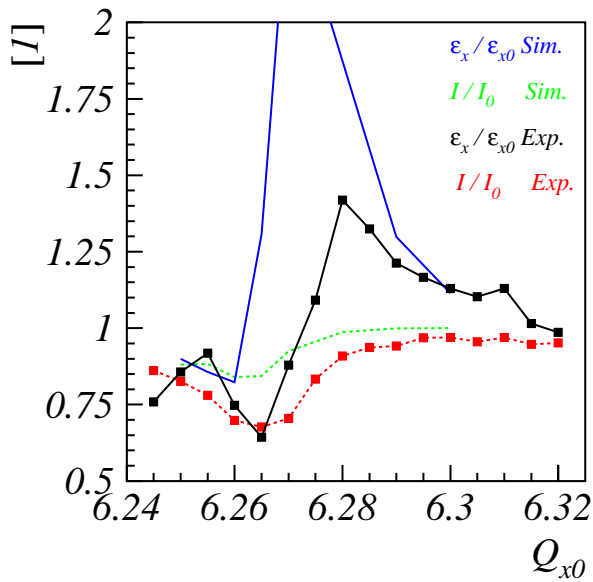


Figure 4: Measurements in the CERN-PS experiment and simulation. In black and blue are drawn the measured and simulated relative emittance growth; in red and green the measured and simulated relative growth.

beam loss) is still below the measurement (maximum beam loss of 32%), but the role of the chromaticity is important: without it only 8% beam loss appears in the simulations. Note also that in the emittance growth regime the horizontal emittance is larger than the measured one. We explain this result in terms of beam loss, in fact in the experiment in the tune range  $6.28 < Q_{x0} < 6.3$  beam loss are detected, therefore damping the emittance growth (especially close  $Q_{x0} = 6.28$ ). The still remaining discrepancy of 16% between measured beam loss and simulated stems from some

of the assumption in the physics-modeling as the code-code benchmarking has proven that code errors should be excluded in this time scale. The main assumption to be validated concerns the self-consistency.

### ESTIMATES OF THE IMPACT OF SELF-CONSISTENCY

The assumption of using a frozen bunch distribution plays an important role in the beam loss prediction. The inconsistency of the frozen model is evident when beam loss reaches, for instance, 20-30% of the initial intensity at once. Less obvious is the impact of beam loss as dynamical process on the trapping of particles. In order to show the relevance of the self-consistency in the long term prediction we made a simulation in which we used a constant focusing model of the CERN-PS ring. We reproduced similar conditions as in the experiment. The space charge modeling is taken analytic from an axi-symmetric bunched beam as the 4th resonance acts mainly on the horizontal plane. In Fig. 5 the green dots show the results of the beam loss when the simulation is pushed to  $2 \times 10^6$  turns: the chromaticity is included but the distribution is kept frozen. Note that the maximum beam loss reaches  $\sim 21\%$  (in  $2 \times 10^6$  turns). The black curve is instead

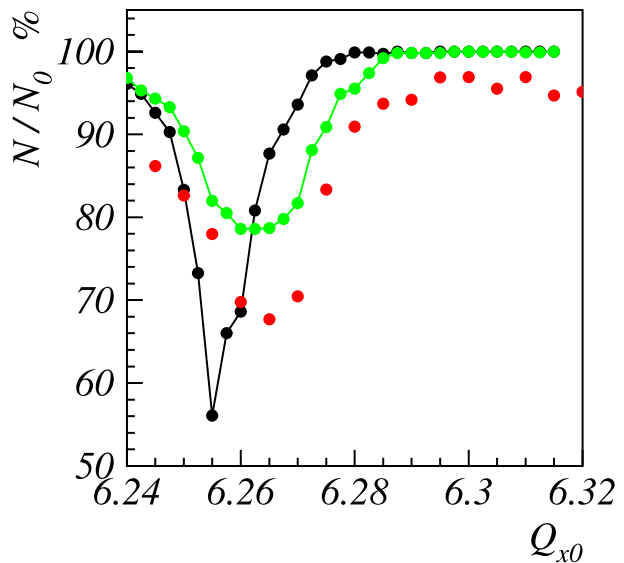


Figure 5: Simulation of the CERN-PS experiment: the green dots are made including the chromaticity and the simulation is up to  $2 \times 10^6$ . With red dots are marked the measurements. In black are the results with artificial perveance reduction.

obtained by adding in an artificial way the effect of beam loss on the space charge through the perveance  $K$ , which is then reduced according to the beam loss. Note that the beam loss over  $4.5 \times 10^5$  turns near  $Q_{x0} = 6.25$  is larger than the experimental findings. This stems from the not

accurate modelization of the self-consistency. This example shows how relevant is the effect of the self-consistency on the beam loss: combined together with the chromaticity it enhances considerably the beam loss much more than a very long term effect without it (see Fig. 5). For understanding the shape of the beam loss in Fig. 5 we first attempt to characterize Fig. 4 (for the frozen model). For this purpose we define the parameter  $\mathcal{R} = (Q_{x0} - Q_{xr})/\Delta Q_x$ , which specifies the distance of the resonance rescaled with respect to the tuneshift. The parameter  $\mathcal{R}$  may be thought to be a rescaling factor in  $Q_{x0} - Q_{xr}$  in Fig. 4 according to the space charge tune-spread of the beam considered. In the frozen model the asymptotic beam loss is depending mainly on  $\mathcal{R}$ . The bunch space charge tune-spread plays a role mainly in determining the time-scale in which the asymptotic loss is reached. Therefore in a self consistent simulation, while beam loss occurs, the ratio  $\mathcal{R} = (Q_{x0} - Q_{xr})/\Delta Q_x$  changes increasing  $\mathcal{R}$ . The upper limit reachable is  $\mathcal{R} \leq 1$ . In fact when  $\mathcal{R} > 1$  the tune-spread does not overlap anymore with the resonance, therefore as  $\mathcal{R}$  approaches to unity beam loss will stop. The integrated effect on beam loss of the change of  $\mathcal{R}$  is difficult to assess. In fact, if the change of  $\mathcal{R}$ , due to beam loss, is too fast then there is not time enough for the beam loss associated to each  $\mathcal{R}$  to buildup: this is shown in Fig. 5 in the range  $6.26 < Q_{x0} < 6.28$ . There the "self-consistent" beam loss (black curve) exhibits less beam loss than the measurements (red curve). The best circumstance to obtain the maximum loss occurs for  $Q_{x0}$  close to the resonance. In this case the asymptotic beam loss is small, consequently  $\mathcal{R}$  will change value very slowly and there is time for the beam loss associated to each  $\mathcal{R}$  to accumulate. This is visible in Fig. 5 were for  $Q_{x0}$  close to the resonance the maximum beam loss of 45% is detected (black curve). The asymmetry of the beam loss vs.  $Q_{x0}$  stems from this effects.

## CONCLUSION/OUTLOOK

The present status of the long term simulation of high intensity beams has reached the border of the needs for self-consistency. After several studies of the effect of trapping of particles into resonances, and the evaluation of the impact of the chromaticity on beam loss, we find here the evidence that the effect of the self-consistency plays an essential role in increasing the beam loss and therefore for validation of physics/code modeling. The self-consistency introduced in this paper is a preliminary attempt to introduce this effect into simulations and the results here presented should not be understood as final. The introduction of the self-consistency into semi-analytical model requires further studies. We add that at GSI an experiment (S317) on the long term effect on a high intensity will be performed in December 2006. From this experiment new data obtained in a controlled experimental condition will be obtained. The use of the rest gas monitor will allow to follow the transverse bunch evolution during storage. A si-

multaneous transverse/longitudinal bunch data acquisition will provide a unique source of benchmarking data.

Work supported by EU design study (contract 515873-DIRACsecondary-Beams).

## REFERENCES

- [1] S. Henderson *et al.*, EPAC, TUPLT170, (2004).
- [2] J. Holmes *et al.*, these Proceedings.
- [3] A. Molodjontsev, ICFA-HB2006, WEAX02, (2006).
- [4] P. Spiller, ICFA-HB2006, MOBP02, (2006).
- [5] G. Franchetti *et al.*, Phys. Rev. ST Accel. Beams **6**, 124201 (2003); E. Metral *et al.*, NIM A **561**, 257 (2006).
- [6] J. Struckmeier Phys. Rev. E **54**, 830 (1996).
- [7] A. Bazzani *et al.* Inst. of Phys. **175**, 25 (2002).
- [8] F. Zimmermann EPAC, WEPCH141 (2006). See also [http://orweb.cern.ch:9000/pls/hhh/code\\_website\\_disp\\_allcat](http://orweb.cern.ch:9000/pls/hhh/code_website_disp_allcat)
- [9] I. Hofmann *et al.* PAC 2005, 330.
- [10] Kellog, *Foundation of Potential Theory* (Dover Publications, New York, USA, 1953), p. 192.
- [11] A. Orzhekhovskaya, G. Franchetti, these Proceedings.
- [12] G. Franchetti, I. Hofmann, ICFA-HB2006, WEAX01, (2006).
- [13] G. Franchetti, I. Hofmann, S. Machida, ICFA-HB2006, THBW01, (2006). See also [http://www-linux.gsi.de/~giuliano/research\\_activity/trapping\\_benchmarking/main.html](http://www-linux.gsi.de/~giuliano/research_activity/trapping_benchmarking/main.html).